Available online at www.sciencedirect.com

SCIENCE DIRECT®

Lithos 77 (2004) 1–19

LITHOS

www.elsevier.com/locate/lithos

The trace element composition of silicate inclusions in diamonds: a review

Thomas Stachel[a,*], Sonja Aulbach[b,c], Gerhard P. Brey[b], Jeff W. Harris[d], Ingrid Leost[b], Ralf Tappert[a,b], K.S. (Fanus) Viljoen[e]

[a] *Department of Earth and Atmospheric Sciences, University of Alberta, Edmonton, AB, Canada T6G 2E3*
[b] *Institut für Mineralogie, Universität Frankfurt, 60054 Frankfurt, Germany*
[c] *GEMOC, Macquarie University, Sydney, NSW 2109, Australia*
[d] *Division of Earth Sciences, University of Glasgow, Glasgow G12 8QQ, UK*
[e] *De Beers GeoScience Centre, P.O. Box 82232, Southdale 2135, South Africa*

Received 27 June 2003; accepted 17 February 2004
Available online 1 June 2004

Abstract

On a global scale, peridotitic garnet inclusions in diamonds from the subcratonic lithosphere indicate an evolution from strongly sinusoidal REE_N, typical for harzburgitic garnets, to mildly sinusoidal or "normal" patterns (positive slope from $LREE_N$ to $MREE_N$, fairly flat $MREE_N$–$HREE_N$), typical for lherzolitic garnets. Using the Cr-number of garnet as a proxy for the bulk rock major element composition it becomes apparent that strong LREE enrichment in garnet is restricted to highly depleted lithologies, whereas flat or positive LREE–MREE slopes are limited to less depleted rocks. For lherzolitic garnet inclusions, there is a positive relation between equilibration temperature, enrichment in MREE, HREE and other HFSE (Ti, Zr, Y), and decreasing depletion in major elements. For harzburgitic garnets, relations are not linear, but it appears that lherzolite style enrichment in MREE–HREE only occurs at temperatures above 1150–1200 °C, whereas strong enrichment in Sr is absent at these high temperatures. These observations suggest a transition from melt metasomatism (typical for the lherzolitic sources) characterized by fairly unfractionated trace and major element compositions to metasomatism by CHO fluids carrying primarily incompatible trace elements. Melt and fluid metasomatism are viewed as a compositional continuum, with residual CHO fluids resulting from primary silicate or carbonate melts in the course of fractional crystallization and equilibration with lithospheric host rocks.

Eclogitic garnet inclusions show "normal" REE_N patterns, with LREE at about 1 × and HREE at about 30 × chondritic abundance. Clinopyroxenes approximately mirror the garnet patterns, being enriched in LREE and having chondritic HREE abundances. Positive and negative Eu anomalies are observed for both garnet and clinopyroxene inclusions. Such anomalies are strong evidence for crustal precursors for the eclogitic diamond sources. The trace element composition of an "average eclogitic diamond source" based on garnet and clinopyroxene inclusions is consistent with derivation from former oceanic crust that lost about 10% of a partial melt in the garnet stability field and that subsequently experienced only minor reenrichment in the most incompatible trace elements. Based on individual diamonds, this simplistic picture becomes more complex, with evidence for both strong enrichment and depletion in LREE.

Trace element data for sublithospheric inclusions in diamonds are less abundant. REE in majoritic garnets indicate source compositions that range from being similar to lithospheric eclogitic sources to strongly LREE enriched. Lower mantle sources, assessed based on CaSi–perovskite as the principal host for REE, are not primitive in composition but show moderate to strong

* Corresponding author.
E-mail address: tstachel@ualberta.ca (T. Stachel).

0024-4937/$ - see front matter
doi:10.1016/j.lithos.2004.03.027

LREE enrichment. The bulk rock $LREE_N$–$HREE_N$ slope cannot be determined from CaSi–perovskites alone, as garnet may be present in these shallow lower mantle sources and then would act as an important host for HREE. Positive and negative Eu anomalies are widespread in CaSi–perovskites and negative anomalies have also been observed for a majoritic garnet and a coexisting clinopyroxene inclusion. This suggests that sublithospheric diamond sources may be linked to old oceanic slabs, possibly because only former crustal rocks can provide the redox gradients necessary for diamond precipitation in an otherwise reduced sublithospheric mantle.

Keywords: Inclusion in diamond; REE; Metasomatism; Lithosphere; Garnet; Majorite; Lower mantle; Subduction

1. Introduction

In a first study of REE patterns of inclusions in diamonds, Shimizu and Richardson (1987) analyzed two harzburgitic garnets from Finsch and Kimberley Pool Mines. Little more trace and ultra trace element measurements were published until the 6th International Kimberlite Conference in 1995. Subsequently, garnet inclusions were recognized as the most useful mineral from which to obtain REE information and a number of studies included trace element analyses obtained mainly by SIMS (ion microprobe) and, more recently, also by laser ablation ICP-MS (e.g., Kaminsky et al., 2001; Davies et al., 2004). So far, these data have been interpreted in the context of their specific diamond sources only. For the purpose of this review, we have compiled a data base of major and trace element analyses for inclusions in diamonds worldwide representing both the lithospheric mantle and sublithospheric sources (asthenosphere, transition zone and lower mantle). The data base is used to constrain the evolution of these lithospheric and sublithospheric source rocks and to examine the possible presence of fluids or melts during diamond formation.

1.1. Data base

For the peridotitic suite a data set of 145 major and trace element analyses of garnet inclusions was assembled. Trace element data on peridotitic clinopyroxene inclusions are still fairly scarce (e.g., Hutchison, 1997; Stachel and Harris, 1997a; Stachel et al., 1999, 2000a; Wang et al., 2000b; Wang and Gasparik, 2001), principally because clinopyroxenes are rare as inclusions in diamond. Furthermore, they are restricted to the lherzolitic (and wehrlitic) inclusions paragenesis and therefore cannot be used to constrain differences and similarities between harzburgitic and lherzolitic diamond sources. Thus, peridotitic clinopyroxene analyses are not included here.

Outliers are a common problem with analytical data bases: a few exotic samples with extreme compositions determine the scale of most plots, making it virtually impossible to display compositional variations affecting the bulk of the samples. We therefore filtered the garnet data base using exceptionally high and low Nd and Ho (both are turning points of sinusoidal patterns) concentrations to exclude 10 aberrant samples. The remaining 135 garnet analyses (100 harzburgitic, 35 lherzolitic) represent diamonds from the Siberian Craton (Aikhal, Mir and Udachnaya: Shimizu et al., 1997), the Sino-Korean Craton (Wang et al., 2000b), the Kalahari Craton including the Kaapvaal Block (Jwaneng: Stachel et al., 2004; Namibian placer deposits: Harris et al., 2004), the Limpopo Belt (Venetia, this study) and the Zimbabwe Block (Orapa: Stachel et al., 2004), the East African Craton (Mwadui: Stachel et al., 1999), the West African Craton (Birim deposits, Ghana: Stachel and Harris, 1997a; Kankan deposits, Guinea: Stachel et al., 2000a), the Guayana Shield, Brazil (Boa Vista: Tappert et al., 2004) and the Slave Craton (Panda: Tappert et al., 2004; DO-27: Davies et al., 2004). The data set covers the compositional space observed for garnet inclusions worldwide with the exception that no garnets with less than 4 wt.% Cr_2O_3 have been analyzed so far (Fig. 1).

For the eclogitic inclusion suite, after exclusion of four aberrant analyses (see above), an analytical data set comprising 39 garnet and 22 clinopyroxene inclusions was established. The samples are derived from the Siberian Craton (Mir and Udachnaya: Taylor et al., 1996), the Kalahari Craton (Jwaneng: Stachel et al., 2004; Namibian placer deposits: this study; Venetia: Aulbach et al., 2002), the East African Craton (Mwadui: Stachel et al., 1999), the

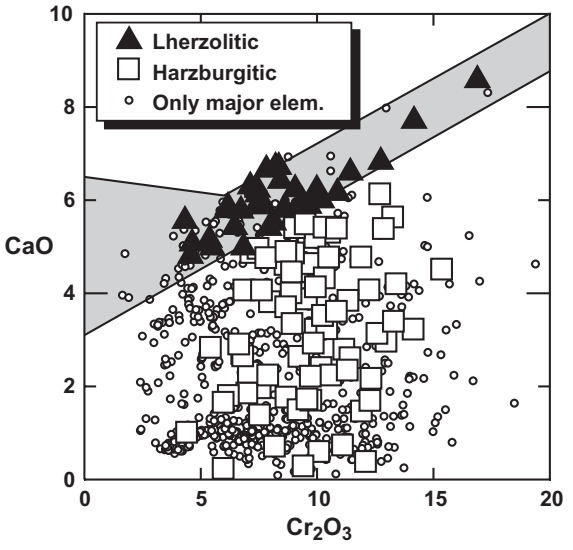

Fig. 1. CaO vs. Cr_2O_3 (wt.%) in garnet. The harzburgitic and lherzolitic garnets in the trace element data base almost completely span the compositional ranges observed for garnet inclusions worldwide (for references see Stachel and Harris, 1997b; Stachel et al., 2000a), with the exception that trace element data are absent for garnet with Cr_2O_3 <4 wt.%. The outline of the lherzolite field (shaded area) is taken from Sobolev et al. (1973).

West African Craton (Kankan deposits, Guinea: Stachel et al., 2000a), the Guayana Shield (Boa Vista: Tappert et al., 2004) and the Slave Craton (DO-27: Davies et al., 2004).

Major and trace element analyses for 15 majoritic garnet inclusions from the asthenosphere and transition zone were obtained for Monastery (Moore et al., 1991), Juina-São Luiz (Wilding, 1990; Harte, 1992; Kaminsky et al., 2001) and Kankan (Stachel et al., 2000a). Trace element analyses of 13 lower mantle CaSi–perovskites are available for Juina-São Luiz (Hutchison, 1997; Harte et al., 1999; Kaminsky et al., 2001) and Kankan (Stachel et al., 2000b).

Previously unpublished data for peridotitic inclusions in diamonds from Venetia (Table 1) and eclogitic inclusions from the placer deposits along the Namibian coast (Table 2) were obtained at the IMS-4f ion probe facility at the University of Edinburgh. Analytical procedures and precision are the same as described in Stachel and Harris (1997a) and Harte and Kirkley (1997). Major elements were determined by electron microprobe analysis (for analytical details, see Stachel et al., 2000a).

2. Peridotitic suite

Garnet inclusions of the peridotitic suite can be further subdivided into a harzburgitic and a lherzolitic paragenesis based on their Ca and Cr contents (Fig. 1, Sobolev et al., 1973; Gurney, 1984). Based on this subdivision, Fig. 2 shows that harzburgitic garnet inclusions are characterized by sinusoidal REE_N patterns ($_N$ stands for normalization to the C1-chondrite composition of McDonough and Sun, 1995), whereas lherzolitic garnets show both sinusoidal and "normal" patterns. Normal patterns—positive slope within the $LREE_N$, flat and enriched $MREE_N$–$HREE_N$—are typical for lherzolitic garnet from mantle xenoliths (Stachel et al., 1998), in particular from sheared peridotites (Shimizu, 1975) and in off-craton occurrences (Hoal et al., 1994).

Hoal et al. (1994) and Shimizu et al. (1997) explained sinusoidal REE_N patterns with disequilibrium models involving modification of preexisting garnet or precipitation from a supersaturated melt. An essential prerequisite for these disequilibrium models is that diffusion of REE in garnet decreases significantly from LREE to HREE. However, Van Orman et al. (2002) showed experimentally (at 2.8 GPa and 1200–1450 °C) that diffusion coefficients for Ce, Sm, Dy, and Yb in pyrope garnet are indistinguishable from each other within analytical uncertainty. Normalization of REE concentrations to a primitive garnet composition (Fig. 3) reveals that sinusoidal garnet patterns are less complex than apparent from normalization to C1-chondrite. The steep positive slope within chondrite normalized LREE is an artifact of rapidly increasing compatibility within the garnet structure due to decreasing ionic radius. Compared to garnet from primitive mantle, average harzburgitic and lherzolitic garnets have LREE enriched, V-shaped REE-patterns and lherzolitic garnets with flat $MREE_N$–$HREE_N$ (e.g., from the Birim deposits in Ghana) actually approach a primitive trace element composition. In addition to the recognition of constant diffusion speeds for LREE and HREE in garnet (Van Orman et al., 2002), the consistency of certain characteristics, such as a fixed turning point at Er over a large compositional range from highly depleted to almost primitive compositions (Fig. 3) clearly is not in support of disequilibrium models either.

Table 1
Major (EPMA) and trace element analyses (SIMS) of peridotitic garnet and clinopyroxene inclusions from Venetia (South Africa)

Sample	V-64a	V-87b	V-95	V-112a	V-149	V-167b	V-167c	V-169a	V-175a	V-175b	V-175c	V-195a	V-197ab
Mineral	Garnet	Garnet	Garnet	Garnet	Cpx	Garnet	Cpx	Garnet	Cpx	Cpx	Cpx	Garnet	Garnet
Assembly	Grt, 2ol	Grt, ol	Grt	Grt, 2ol	Cpx	Grt, Cpx	Grt, cpx	Grt	3cpx, opx	3cpx, opx	3cpx, opx	2grt, ol	Grt, ol
P_2O_5	0.01	0.08	≤0.01	0.07	≤0.01	0.06	≤0.01	0.03	≤0.01	≤0.01	≤0.01	0.03	0.02
SiO_2	41.87	40.79	41.03	39.56	55.17	41.78	54.72	40.95	55.17	54.80	55.30	41.76	41.24
TiO_2	≤0.01	0.10	0.09	0.05	0.08	0.23	0.04	0.20	0.08	0.06	0.08	0.61	0.10
Al_2O_3	17.65	11.91	17.49	10.16	1.46	19.85	1.34	14.81	1.23	1.23	1.22	17.04	15.92
Cr_2O_3	9.40	14.75	9.21	18.49	1.58	4.63	0.83	11.43	1.04	0.86	1.04	7.85	9.06
FeO	4.30	5.52	6.41	5.47	3.27	5.92	2.79	5.07	2.42	2.70	2.46	4.98	6.33
MnO	0.20	0.27	0.34	0.31	0.13	0.28	0.13	0.23	0.11	0.11	0.10	0.25	0.30
NiO	≤0.01	0.01	≤0.01	≤0.01	0.07	0.02	0.08	0.02	0.06	0.07	0.06	0.01	0.02
MgO	25.94	20.79	22.92	23.23	18.10	21.78	19.89	20.38	19.19	21.05	19.68	22.37	20.11
CaO	0.29	6.06	2.64	1.64	18.37	5.07	18.23	6.59	18.85	17.14	18.28	4.24	6.23
Na_2O	≤0.01	0.03	0.03	≤0.01	1.20	0.03	0.90	0.03	0.84	0.75	0.81	0.05	0.02
K_2O	≤0.01	≤0.01	≤0.01	≤0.01	0.07	≤0.01	0.15	≤0.01	0.05	0.04	0.06	≤0.01	≤0.01
Total	99.66	100.30	100.18	98.99	99.51	99.65	99.08	99.74	99.05	98.82	99.08	99.19	99.35
Ti	14.20	602.00	463.00	327.00	453.00	1130.00	218.00	1140.00	351.00	351.00	363.00	3300.00	547.00
Sr	9.97	3.42	0.42	31.30	177.00	0.89	168.00	0.63	39.80	40.80	41.60	8.30	0.47
Y	0.29	2.22	1.63	2.25	0.78	4.30	0.35	4.07	0.80	0.79	0.82	24.30	2.24
Zr	1.63	29.40	27.90	24.20	0.90	13.20	0.38	15.40	0.32	0.31	0.29	119.00	1.54
Nb	0.16	8.52	0.49	0.67	0.51	6.00	1.49	4.25	0.42	0.46	0.53	0.45	1.94
Ba	0.02	0.01	0.02	0.08	0.69	0.04	2.28	0.01	1.80	1.31	2.87	0.01	0.01
La	0.44	0.45	0.01	0.74	3.00	0.34	8.91	0.20	1.01	0.98	1.32	0.23	0.06
Ce	5.33	4.05	0.16	21.60	8.74	2.34	21.90	1.60	1.59	1.76	2.05	2.48	0.76
Pr	1.17	1.28	0.08	7.88	1.30	0.57	2.54	0.38	0.22	0.21	0.28	0.82	0.24
Nd	6.12	11.30	0.89	39.50	6.06	3.57	9.42	3.87	1.36	1.32	1.37	8.01	1.89
Sm	0.73	4.89	0.55	3.42	0.74	0.89	0.86	2.61	0.30	0.35	0.49	4.66	0.36
Eu	0.11	1.71	0.22	0.72	0.22	0.28	0.21	0.85	0.12	0.12	0.10	1.83	0.10
Gd	0.40	3.60	0.88	2.71	0.43	0.74	0.31	2.07	0.36	0.39	0.32	6.35	0.23
Tb	0.01	0.32	0.10	0.21	0.07	0.15	0.05	0.20	0.06	0.07	0.03	0.96	0.04
Dy	0.05	0.87	0.55	1.16	0.36	0.75	0.04	0.98	0.16	0.27	0.36	5.83	0.36
Ho	0.01	0.15	0.08	0.12	0.04	0.17	0.02	0.15	0.04	0.04	0.05	1.13	0.09
Er	0.04	0.35	0.17	0.20	0.02	0.57	0.04	0.65	0.13	0.16	0.11	2.96	0.39
Yb	0.09	0.56	0.18	0.08	n.a.	0.90	n.a.	0.80	n.a.	n.a.	n.a.	2.24	0.68
Lu	0.04	0.09	0.06	0.01	0.01	0.13	0.00	0.15	0.00	0.01	0.01	0.28	0.15
Hf	0.02	0.58	0.66	0.40	0.07	0.41	0.05	0.25	0.03	0.01	0.04	2.47	0.05

Trace element concentrations are given in wt. ppm and are rounded to the second decimal place, concentrations of 0.00 ppm therefore refer to values < 0.005 ppm. "n.a." stands for "not analyzed".

Thus, only three hypotheses for the origin of peridotitic REE patterns are further considered: (i) the patterns are an inherent characteristic of cratonic garnet peridotites, related to their primary formation; (ii) they are the result of a reenrichment event that also modified the major element composition of these rocks, i.e., melt infiltration; or (iii) they were caused by fluid metasomatism involving CHO agents enriched in incompatible trace elements, but without significant impact on major elements.

2.1. Relationship between garnet trace element and bulk rock major element composition

The first two hypotheses outlined above require that discernible correlations between major and trace element compositions exist. The Cr/Al ratio (or Cr content) of garnet is a measure of the Cr/Al ratio of the source rock which in turn is a proxy for the degree of depletion in major elements. Griffin et al. (1999a) have shown that this relationship is sufficiently strong to employ Cr in garnet to predict the major element

Table 2
Major (EPMA) and trace element analyses (SIMS) of eclogitic garnet and clinopyroxene inclusions from Namibia (alluvial mines along the Orange River close to Oranjemund, along the Namibian coast to Elisabeth Bay and from Namibian offshore deposits)

Sample	Nam-13	Nam-34	Nam-35	Nam38	Nam-38	Nam-43	Nam-47	Nam-5	Nam-59	Nam-63	Nam-68	Nam74
Mineral	Garnet	Cpx	Garnet	Garnet	Cpx	Cpx	Garnet	Garnet	Garnet	Garnet	Garnet	Garnet
P_2O_5	0.05	0.01	0.14	0.03	0.01	≤0.01	0.03	0.14	0.04	0.05	0.05	0.08
SiO_2	39.43	53.55	39.10	39.67	54.71	54.52	40.79	39.78	39.37	40.30	38.73	39.41
TiO_2	0.67	0.53	1.14	0.17	0.16	0.26	0.24	1.01	0.30	0.53	0.36	0.30
Al_2O_3	22.18	7.92	20.81	22.92	6.29	4.12	22.80	21.52	21.98	21.95	22.12	22.92
Cr_2O_3	0.03	0.05	0.02	0.19	0.18	0.10	0.14	0.15	0.06	0.18	0.04	0.04
FeO	15.37	6.41	21.76	19.75	6.51	7.08	15.57	15.93	22.48	19.23	19.67	19.24
MnO	0.27	0.07	0.41	0.43	0.18	0.21	0.34	0.29	1.02	0.40	0.67	0.23
NiO	≤0.01	0.03	≤0.01	0.01	≤0.08	0.02	0.01	≤0.01	≤0.01	≤0.01	≤0.01	≤0.01
MgO	7.35	10.11	6.95	14.34	12.71	14.93	16.41	10.52	9.21	13.77	8.98	10.89
CaO	14.36	15.70	9.74	2.66	11.92	15.42	3.59	10.41	5.86	3.66	8.45	6.59
Na_2O	0.25	4.19	0.37	0.09	4.18	2.43	0.15	0.40	0.17	0.14	0.18	0.17
K_2O	≤0.01	0.26	≤0.01	≤0.01	0.49	0.13	≤0.01	≤0.01	≤0.01	≤0.01	≤0.01	≤0.01
Total	99.96	98.83	100.45	100.26	97.42	99.20	100.07	100.16	100.49	100.21	99.26	99.88
Sr	2.27	134.00	3.42	0.37	169.00	81.20	0.29	3.26	3.69	0.50	4.78	1.50
Y	42.90	1.57	47.10	33.35	8.03	6.72	11.20	39.50	21.20	37.10	20.40	68.30
Zr	49.20	20.00	63.60	2.10	7.79	7.78	7.98	176.00	9.70	25.30	17.80	69.20
Nb	0.00	0.14	0.00	0.04	0.00	0.00	0.00	0.19	0.00	0.00	0.00	0.00
Ba	0.07	0.84	0.01	3.22	19.00	5.93	0.00	0.01	0.02	0.18	0.05	0.00
La	0.02	1.96	0.10	0.06	6.88	1.16	0.00	0.10	0.05	0.03	0.16	0.28
Ce	0.38	6.02	1.05	0.15	12.00	2.50	0.03	1.98	0.43	0.16	0.85	2.78
Pr	0.15	1.17	0.43	0.04	1.40	0.54	0.02	0.91	0.13	0.07	0.26	0.77
Nd	1.55	7.08	4.17	0.47	7.45	2.94	0.14	9.30	1.50	1.17	3.15	6.80
Sm	1.62	1.62	2.80	0.64	2.77	1.52	0.23	5.22	1.76	1.19	2.92	4.31
Eu	0.94	0.45	1.33	0.44	0.91	0.48	0.10	1.48	0.92	0.47	1.47	1.34
Gd	4.95	0.98	5.25	2.04	4.95	2.44	0.50	7.32	2.62	2.52	4.13	8.56
Tb	1.22	0.09	1.16	0.64	0.50	0.28	0.14	1.31	0.55	0.70	0.72	1.91
Dy	8.49	0.44	8.50	5.27	2.57	1.47	1.56	8.10	3.62	6.03	3.98	12.80
Ho	1.93	0.09	1.90	1.28	0.40	0.37	0.45	1.67	0.86	1.38	0.85	2.72
Er	5.40	0.09	6.14	4.20	0.73	0.77	1.89	5.01	2.30	4.45	2.39	8.48
Yb	5.39	n.a.	7.44	5.11	n.a.	n.a.	2.91	4.75	2.99	5.98	2.12	10.00
Lu	0.65	0.01	1.11	0.82	0.06	0.07	0.46	0.68	0.38	0.86	0.30	1.47

Sample	Nam-78	Nam-80	Nam-86	Nam-89	Nam-89	Nam-102	Nam-202	Nam-202	Nam-203	Nam-203	Nam-205	Nam-207
Mineral	Cpx	Garnet	Garnet	Cpx	Garnet	Cpx	Cpx	Garnet	Cpx	Garnet	Cpx	Cpx
P_2O_5	0.02	0.05	0.04	≤0.01	0.02	0.01	≤0.01	0.00	0.01	0.08	≤0.01	0.02
SiO_2	54.99	40.90	39.59	53.86	40.54	56.81	55.80	37.53	53.62	39.51	54.44	55.78
TiO_2	0.62	0.25	0.58	0.20	0.33	0.43	0.53	0.12	0.46	0.57	0.21	0.45
Al_2O_3	12.51	23.29	22.55	5.50	22.67	19.32	9.66	20.85	7.20	21.00	3.77	6.17
Cr_2O_3	0.03	0.24	0.02	0.10	0.18	0.08	0.09	0.05	0.08	0.10	0.30	0.20
FeO	5.36	8.35	10.53	4.75	13.50	2.79	3.41	30.92	6.54	18.09	5.99	7.22
MnO	0.06	0.13	0.20	0.08	0.31	0.03	0.05	0.60	0.08	0.37	0.10	0.13
NiO	0.01	0.01	≤0.01	0.06	0.02	0.00	0.04	≤0.01	0.03	≤0.01	0.08	0.06
MgO	7.28	14.44	7.57	13.36	14.45	3.97	10.69	1.73	10.45	9.62	15.46	14.13
CaO	11.77	11.89	18.53	17.76	7.87	5.99	13.92	8.60	15.61	9.07	15.82	11.28
Na_2O	6.92	0.12	0.19	2.74	0.10	9.59	5.71	0.02	4.23	0.16	2.12	4.55
K_2O	0.24	≤0.01	≤0.01	0.10	≤0.01	0.10	0.08	≤0.01	0.03	≤0.01	0.59	0.09
Total	99.80	99.68	99.82	98.51	99.97	99.11	99.97	100.42	98.32	98.56	98.89	100.08
Sr	272.00	1.28	3.81	76.20	0.59	44.10	183.35	0.12	79.00	0.83	166.80	200.00
Y	2.46	5.79	22.00	1.04	12.90	1.04	0.54	60.00	1.70	33.00	1.76	8.30

(continued on next page)

Table 2 (*continued*)

Sample	Nam-78	Nam-80	Nam-86	Nam-89	Nam-89	Nam-102	Nam-202	Nam-202	Nam-203	Nam-203	Nam-205	Nam-207
Mineral	Cpx	Garnet	Garnet	Cpx	Garnet	Cpx	Cpx	Garnet	Cpx	Garnet	Cpx	Cpx
Zr	13.70	8.38	77.80	3.41	7.24	28.00	13.52	2.50	31.00	43.00	2.25	46.00
Nb	0.00	0.00	0.00	0.28	0.27	0.00	0.02	0.00	0.00	0.00	1.05	0.10
Ba	0.88	0.06	0.02	0.56	0.04	0.22	27.01	0.02	0.35	0.01	67.28	0.20
La	2.97	0.00	0.03	1.00	0.03	0.38	4.85	0.01	0.27	0.01	19.04	2.10
Ce	8.48	0.00	0.38	3.47	0.30	1.26	8.48	0.02	1.70	0.16	18.94	10.00
Pr	1.40	0.17	0.15	0.50	0.10	0.25	0.98	0.00	0.47	0.11	1.24	2.20
Nd	6.50	0.98	2.23	2.38	0.75	2.13	4.23	0.08	3.80	2.30	4.62	13.00
Sm	1.17	0.54	1.79	0.52	0.59	0.62	0.69	0.30	1.30	2.20	0.58	3.00
Eu	0.33	0.35	1.04	0.19	0.42	0.16	0.20	0.21	0.44	1.10	0.16	0.91
Gd	0.71	1.57	4.04	0.35	1.12	0.48	0.43	3.00	1.20	4.40	0.99	3.20
Tb	0.12	0.25	0.77	0.07	0.32	0.08	0.03	1.50	0.16	0.88	0.10	0.47
Dy	1.05	1.40	5.15	0.26	2.52	0.29	0.23	12.00	0.87	6.90	0.63	2.60
Ho	0.11	0.29	1.03	0.09	0.52	0.05	0.05	2.00	0.10	1.50	0.10	0.45
Er	0.46	0.38	2.41	0.00	1.70	0.12	0.09	4.50	0.30	4.40	0.36	0.94
Yb	n.a.	0.39	1.93	n.a.	2.09	n.a.	n.a.	n.a.	n.a.	n.a.	n.a.	n.a.
Lu	0.01	0.08	0.30	0.00	0.36	0.00	0.02	0.52	0.03	0.80	0.01	0.09

Trace element concentrations are given in wt. ppm and are rounded to the second decimal place, concentrations of 0.00 ppm therefore refer to values < 0.005 ppm. "n.a." stands for "not analyzed".

and modal composition of cratonic garnet peridotites. Thus, the molar Cr-number (100Cr/[Cr + Al]) of garnet inclusions will be used to examine possible correlations between major and trace elements.

The shape of garnet REE_N patterns (Fig. 2) is determined by the existence and position of a peak within the $LREE_N$ and by the slopes (i) within the $LREE_N$, (ii) from $LREE_N$ to $MREE_N$ (MREE: Sm–Ho) and (iii) from $MREE_N$ to $HREE_N$. The actual concentrations of REE are less diagnostic as they will be strongly influenced by the amount of modal garnet present. In addition, for lherzolitic garnets LREE concentrations (and consequently, ratios of LREE to MREE and HREE) will be influenced by the presence of clinopyroxene.

No significant linear correlations between Cr-number and relative and absolute REE concentrations are observed for peridotitic garnets of both parageneses. However, for the harzburgitic garnets it is noted (i) that the highest La (LREE) contents occur at Cr-numbers greater than 25 (Fig. 4) and (ii) that enrichment in MREE and Y (i.e., positive $LREE_N$–$MREE_N$ slopes, indicated by superchronditic Y/Nd in Fig. 4), and in HREE is restricted to Cr-numbers below 30 (Fig. 4). The apparent relationship between high Cr-number and high average La content possibly reflects highly depleted rocks with low modal garnet, thus being very sensitive to metasomatic modification. Such effects may have been enhanced by a moderate increase in garnet/liquid distribution coefficients for LREE with increasing Cr content in garnet (Wang et al., 1998; HREE are not affected).

For the lherzolitic garnets positive slopes from $LREE_N$ to $MREE_N$ (similar to harzburgitic garnets, see Fig. 4) and the highest concentrations in MREE–HREE (from Tb onwards, see Yb in Fig. 4) are restricted to Cr-numbers below 30. The highest contents in strictly incompatible elements such as Ce (LREE) and Sr are found for the three lherzolitic garnets with Cr-numbers above 40. Usually, Sr contents above 2 ppm are restricted to harzburgitic garnets, suggesting that very low modal clinopyroxene (as the principal host of Sr and LREE in lherzolite) in the source of Cr-rich lherzolitic garnets may be the cause of elevated Ce and Sr.

Despite the observation that a few harzburgitic garnets with low Cr-number show distinct MREE–HREE enrichment, the REE_N patterns for most of the harzburgitic paragenesis are independent of the bulk rock major element composition. For lherzolitic garnets, it is evident that positive slopes from $LREE_N$ to $MREE_N$–$HREE_N$ are restricted to less Cr-rich samples, but this relationship does not take the form of a linear correlation and a number of samples with low Cr-number still have sinusoidal patterns.

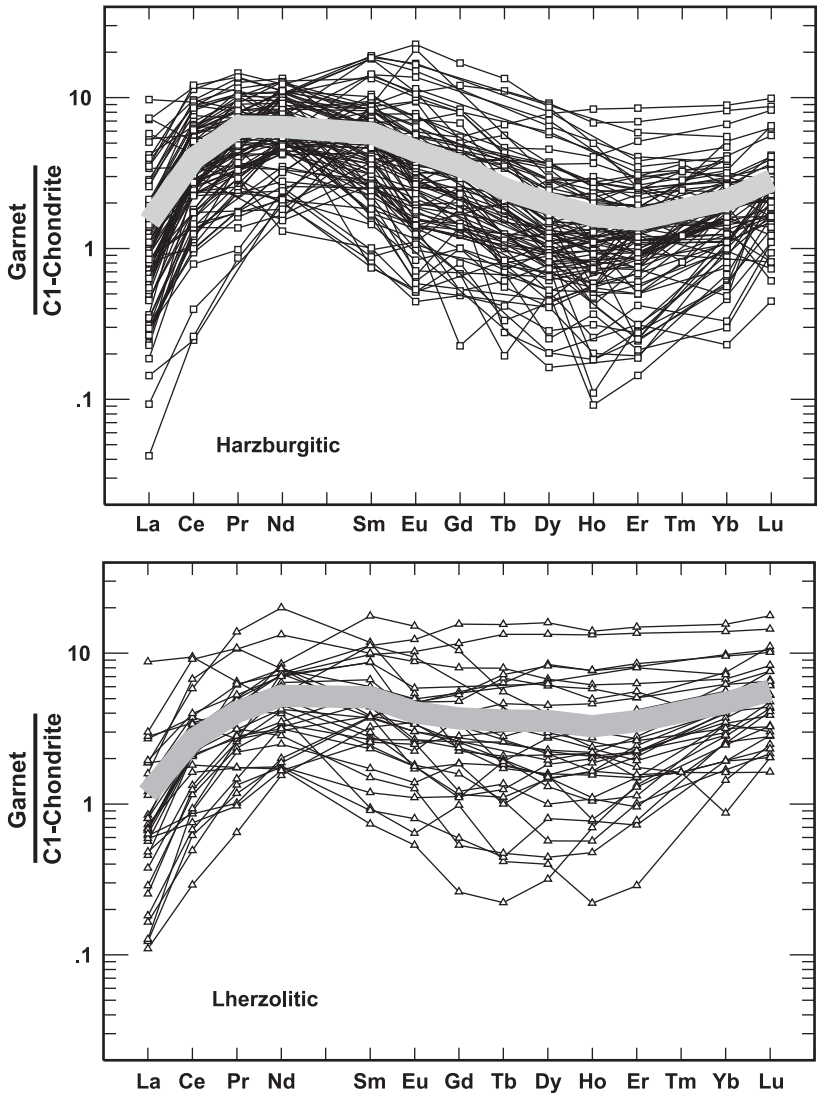

Fig. 2. Chrondrite-normalized REE patterns of harzburgitic and lherzolitic garnet inclusions from worldwide sources. Average compositions are indicated by thick shaded lines. The validity of the calculated average for harzburgitic garnets is difficult to assess from this diagram alone because of a large number of overlapping analyses. However, we have verified from the REE concentrations that we are dealing with unimodal distributions and that the median REE pattern is not significantly different from the average shown above.

As a first conclusion, the absence of linear correlations between the bulk rock major element composition (inferred from the Cr-number of garnet) and garnet REE_N excludes the primary processes (which cause the chemical depletion of the subcratonic lithospheric mantle) as the determining factor for the observed variations in trace composition. This is in agreement with a two-stage model of primary depletion and secondary reenrichment first proposed by Frey and Green (1974). However, for some lherzolitic and a very few harzburgitic garnets, it appears that there is a relationship between MREE–HREE enrichment and decreasing depletion in bulk rock major element composition. The nonlinearity of this relationship may be attributed to variations either in the style of metasomatic overprint or in the degree of primary depletion of

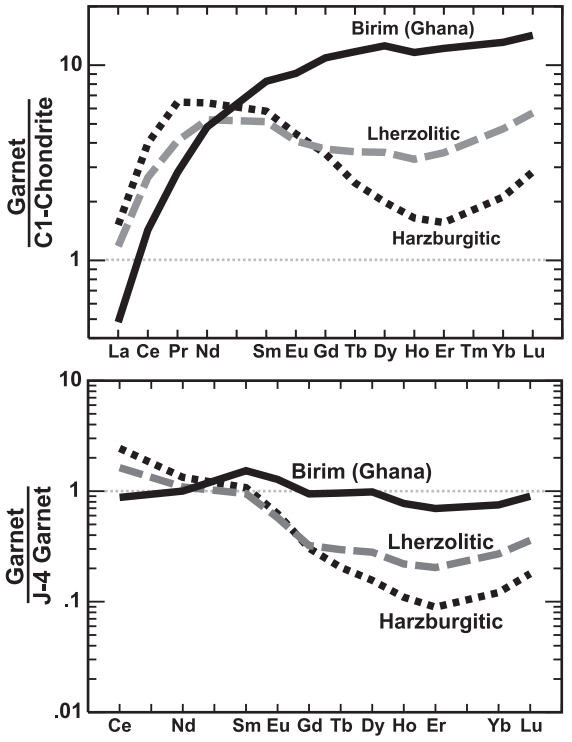

Fig. 3. Average compositions of harzburgitic and lherzolitic garnet inclusions from worldwide sources and of three lherzolitic garnets with "flat" MREE–HREE from the Birim deposits in Ghana (Stachel and Harris, 1997a). The data are normalized to C1-chondrite and to a garnet from a primitive mantle bulk rock composition (J-4 of Jagoutz and Spettel, see Stachel et al., 1998 for details).

the source rock (leading to different starting compositions for metasomatic overprint), or both.

2.2. Garnet composition and equilibration temperature

To test if there is a possible dependence of the style of metasomatic overprint on the thermal regime compositional parameters are plotted against garnet–olivine equilibration temperatures (O'Neill and Wood, 1979; O'Neill, 1980), calculated for a fixed pressure of 5 GPa. For the data base evaluated here, there is a negative correlation between equilibration temperature and Cr-number (Fig. 5) for lherzolitic garnets. This negative correlation is less well developed for harzburgitic garnets where it appears to break down at temperatures below about 1100 °C. This relationship cannot be linked to increased solution of Cr-rich

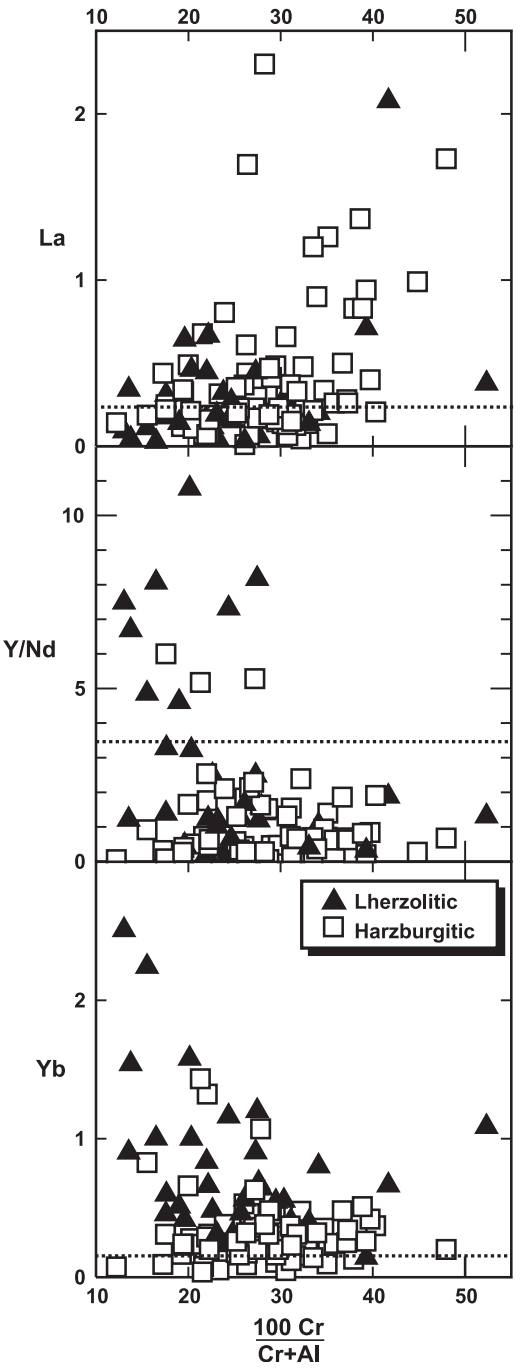

Fig. 4. Covariations of REE (in wt. ppm; Y is used as a substitute for the less abundant MREE) and molar Cr-number of garnet inclusions worldwide. Dotted lines indicate chondritic abundances or, in the case of Y/Nd, the chondritic ratio. Garnets with superchondritic Y/Nd have a positive $LREE_N$–$MREE_N$ slope.

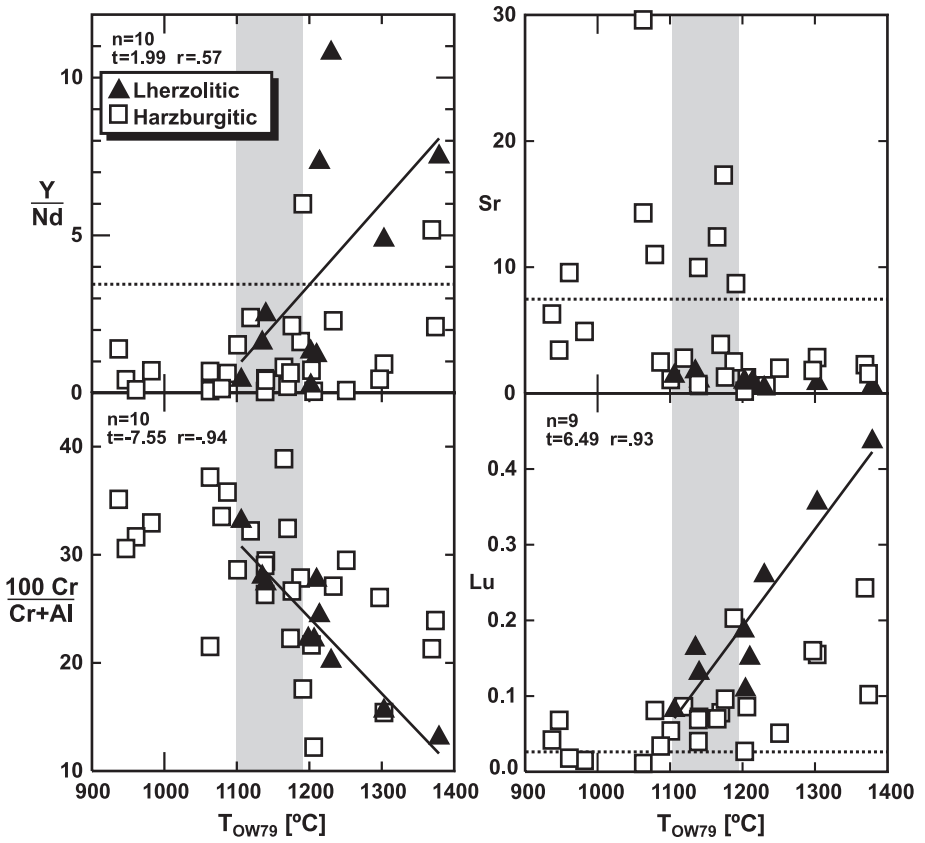

Fig. 5. Covariations between compositional parameters of garnet inclusions and equilibration temperature (calculated from garnet–olivine equilibria for a fixed pressure of 5 GPa). Regression lines are based on lherzolitic inclusions (▲) only. Dotted lines indicate chondritic abundance or ratio. The shaded area indicates the approximate temperature where a change in metasomatic regime appears to take place.

spinel into garnet with increasing pressure and temperature (Doroshev et al., 1997; Grütter and Sweeney, 2000), as this would lead to a positive correlation of temperature and Cr-number. Therefore, a decreasing degree of chemical depletion of the diamond source rocks with increasing temperature is indicated for all samples that formed above about 1100 °C.

For the harzburgitic paragenesis, the fairly crude correlation between increasing temperature and source fertility (Fig. 5) is not accompanied by linear correlations with the garnet trace element composition. However, some nonlinear relationships are observed: high Sr (>3 ppm, see Fig. 5) and Ce (>4 ppm, not shown) are restricted to equilibration temperatures below about 1150–1200 °C, whereas high HREE (Yb>50 ppb and Lu>100 ppb, see Fig. 5) occur only in some of the samples which formed above 1190 °C. A similar relationship exists for the $LREE_N$–$MREE_N$ slope (represented in Fig. 5 by the Y/Nd ratio), where positive slopes for harzburgitic and also for lherzolitic garnets only occur above 1190 °C.

For the lherzolitic garnets where all 10 samples follow a linear relation between temperature and source fertility, positive correlations with equilibration temperature also exist with the MREE–HREE from Eu onwards (the HREE Lu is shown in Fig. 5) and with the other HFSE: Ti, Y and Zr.

2.3. Model

The garnet data indicate that the metasomatic processes reenriching the harzburgitic diamond sources in incompatible trace elements generally show little dependence on equilibration temperature and

leave the major element composition largely unaffected. This suggests metasomatism by CHO fluids with highly fractionated trace element compositions (very high $LREE_N/HREE_N$, see Fig. 6). This interpretation is consistent with the high solidus temperature of harzburgite, which effectively prevents grain boundary percolation of *dry* silicate and carbonate melts at the PT conditions of diamond formation, as they would freeze upon equilibration with the host rock (Nielson and Wilshire, 1993; Stachel and Harris, 1997a). However, the observed nonlinear relationships, i.e., the apparent restriction of strong preferential enrichment in highly incompatible elements (increased Sr and Ce) to harzburgitic sources at temperatures below about 1150–1200 °C, indicate that such highly fractionated fluids may be absent at high temperatures. A few harzburgitic garnets, which all equilibrated at temperatures above 1190 °C, appear to be influenced by "lherzolite style" metasomatism introducing HREE and probably also refertilizing the bulk rock major element composition (all of these garnets have Cr-numbers below 30). Equilibration temperatures are still below the harzburgitic solidus, but these samples may be derived from the vicinity of magmatic intrusions or close to the base of the lithosphere, where silicate melts may penetrate for some distance into harzburgite before they freeze. The observation that harzburgitic garnets show a (poor) linear correlation between equilibration temperature and Cr-number without accompanying trace element trends suggests the possible operation of an additional process which cannot be constrained based on this data set.

The observations for lherzolitic garnet inclusions imply that their sources were affected by metasomatism that increased in intensity with temperature and affected both major and trace elements. This coincides with the fact that diamond formation generally takes place above the "wet" lherzolite solidus (about 1100–1150 °C at 5 GPa in the presence of CHO, e.g., Wyllie, 1987) facilitating percolation of silicate melts along grain boundaries.

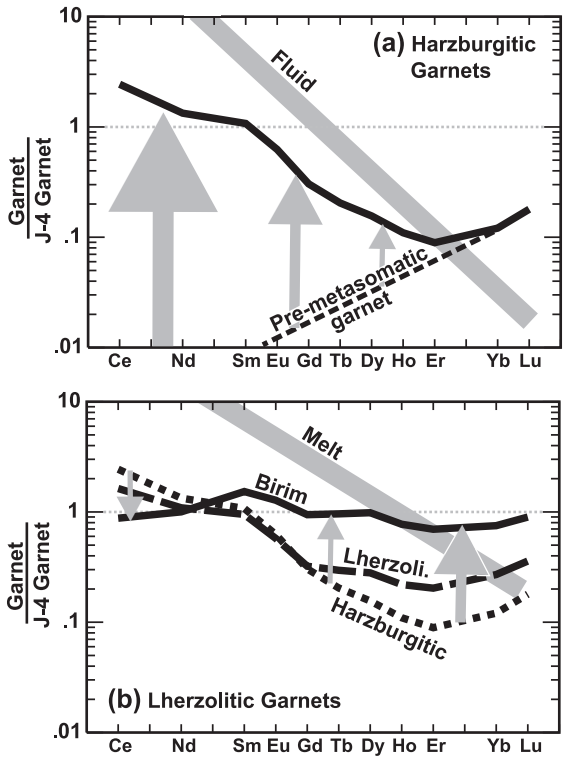

Fig. 6. Schematic illustration of the metasomatic reenrichment affecting harzburgitic and lherzolitic diamond sources. Average garnet compositions are normalized to garnet from a primitive mantle bulk rock composition (see Fig. 3). (a) Harzburgitic garnets have V-shaped patterns with the positive slope within the HREE reflecting the strongly LREE depleted composition of a protolith that experienced a major melt extraction event (c.f. Stachel et al., 1998). The premetasomatic REE pattern of garnet in equilibrium with this protolith is shown as a dashed line. The evolution of the harzburgitic diamond source thus requires interaction with an extremely fractionated metasomatic agent that introduces mainly LREE, comparatively little MREE and almost no HREE. The thick grey line indicates a possible REE pattern for such a fluid. (b) This scenario is based on an origin of lherzolitic diamond sources through metasomatic enrichment of former harzburgite (Stachel et al., 1998; Griffin et al., 1999b). The figure shows a two-stage evolution from harzburgitic garnet (dotted line) to average lherzolitic garnet (dashed line) and finally to fully refertilized lherzolitic garnet (solid line, "Birim") with primitive REE pattern. Transition from harzburgitic to average lherzolitic garnet involves enrichment in MREE and HREE. High garnet–liquid partition coefficients for HREE cause HREE enrichment in garnet even through melts with approximately chondritic HREE abundances. Conversion of harzburgite to lherzolite is accompanied by introduction of increasing modal clinopyroxene which leads to an apparent depletion in LREE relative to harzburgitic garnet. Continuous introduction of melt (approximate composition indicated as a thick grey line) finally leads to garnet that mimics the trace element composition of garnet from primitive mantle. Calculated melt compositions in equilibrium with such "primitive" garnets correspond to typical low-volume mantle melts (e.g., kimberlite, lamproite or MORB source megacryst magma, see Stachel and Harris, 1997a; Burgess and Harte, 1999).

The two styles of metasomatic enrichment identified here (Fig. 6), (i) subsolidus infiltration of strongly fractionated CHO fluids with a very high ratio of LREE to MREE, HREE and other HFSE and (ii) supersolidus percolation of melts that refertilize the diamond sources both in major and trace elements and that are characterized by a moderate enrichment of LREE over MREE, HREE and other HFSE, probably should be viewed as end-members of a compositional continuum rather than two strictly separate processes.

3. Eclogitic suite

The very light carbon isotopic composition of some eclogitic diamonds has been interpreted by numerous authors to reflect diamond formation from subducted organic matter (e.g., Frank, 1969; Kirkley et al., 1991; McCandless and Gurney, 1997). However, high equilibration temperatures of eclogitic inclusions are inconsistent with diamond formation within cold subducting slabs (Gurney, 1989; Stachel et al., 2002) and it appears possible that isotopic fraction-

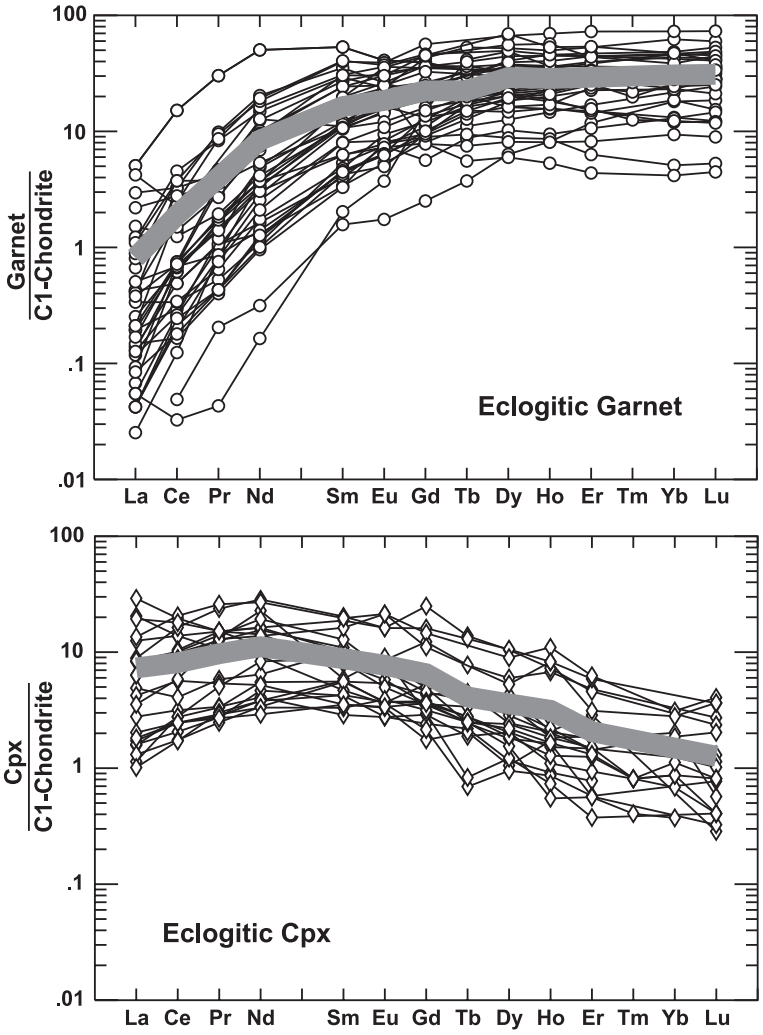

Fig. 7. Chondrite normalized REE concentrations in eclogitic garnet (top) and clinopyroxene inclusions in diamonds from worldwide sources. Average compositions are indicated by thick shaded lines.

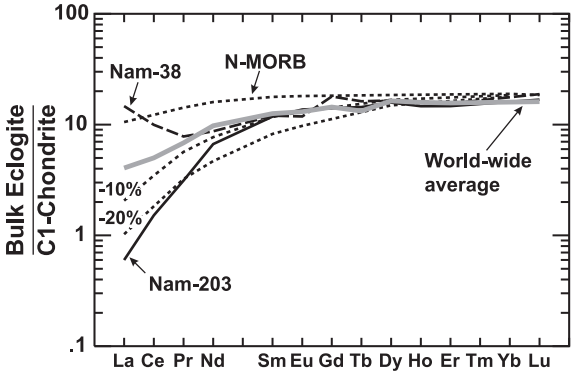

Fig. 8. Based on a garnet–clinopyroxene ratio of 1:1, whole-rock REE patterns are calculated (i) from the average compositions shown in Fig. 7 and (ii) for coexisting garnet–clinopyroxene pairs in two diamonds from Namibia. In addition, the composition of N-MORB is shown together with residues of an original N-MORB composition after 10% and 20% of partial melt were removed in the stability field of eclogite (batch melting with a garnet–cpx residue, assuming a garnet–cpx ratio of 1:1. $D^{Cpx/L}$ from Hart and Dunn, 1993; $D^{Grt/L}$ from Zack et al., 1997).

ation may be the true cause of the observed range in $\delta^{13}C$ (Cartigny et al., 1998), which is conceivable because of the poor buffering capacity of eclogite for hydrous CO_2 fluids (Luth, 1993). Oxygen (e.g., Macgregor and Manton, 1986; Jacob and Foley, 1999; Schulze et al., 2003) and sulfur isotopic analyses (Farquhar et al., 2002) nevertheless provide strong indications that eclogitic diamond sources probably have crustal protoliths. It is generally assumed that cratonic eclogites are not simply the metamorphosed equivalent of Archean seafloor, but that partial melting, probably in the eclogite stability field, lead to chemical depletion (Ireland et al., 1994), thereby explaining the absence of a free SiO_2 phase. Based on REE analyses of garnet and clinopyroxene inclusions in eclogitic diamonds, it is possible to revisit the question of possible oceanic precursors.

Eclogitic garnets (Fig. 7) show REE_N patterns that are similar in shape to the most fertile lherzolitic inclusions (see Fig. 3, Birim garnets), i.e., a steep positive slope within the $LREE_N$ and fairly flat $MREE_N$–$HREE_N$, but at higher MREE–HREE concentrations (averaging at about 30 × chondritic abundance). Eclogitic clinopyroxenes (Fig. 7) have positive slopes within the $LREE_N$, peaking at Nd and then slowly decrease in $MREE_N$ and $HREE_N$ to about chondritic abundance for Lu. This is distinctive from the majority of peridotitic clinopyroxenes which often have negative slopes within the $LREE_N$ and subchondritic Lu. It has been shown that eclogitic diamond sources, after emplacement in the cratonic lithosphere, are affected by both metasomatic overprint and partial melting (e.g., Taylor et al., 1996; Sobolev et al., 1998). However, the overall consistency of the majority of analyses shown in Fig. 7 suggests that metasomatic overprint may not have completely eradicated the primary signature of the eclogitic sources and that perturbations for the bulk of the data may be limited to the most incompatible elements. Assuming that eclogite represents approximately equal proportions of garnet and clinopyroxene, an average source composition can be calculated (Fig. 8, c.f. Ireland et al., 1994) based on the mean compositions shown in Fig. 7. This calculated average composition compares extremely well with an N-MORB precursor that has lost about 10% of a partial melt in the eclogite stability field and that subsequently experienced some reenrichment in LREE. Two eclogitic garnet–clinopyroxene inclusion pairs in diamonds from Namibia may be used to support this interpretation. Both pairs yield similar bulk rock compositions for the MREE and HREE but differ in LREE, with Nam-203 resembling a strongly (ca 20%) melt depleted oceanic protolith and Nam-38 showing the effect of metasomatic reenrichment in LREE.

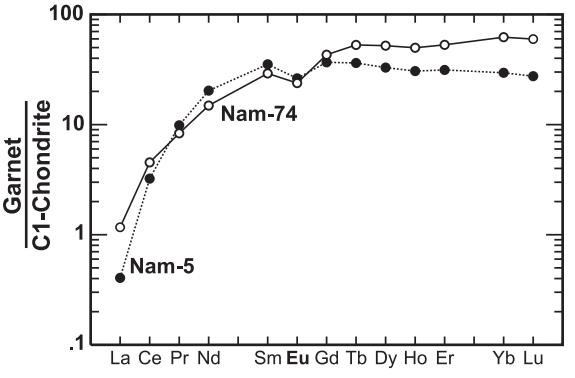

Fig. 9. Negative Eu anomalies in eclogitic garnet inclusions from Namibia. Negative and positive Eu anomalies have also been observed in eclogitic garnet and clinopyroxene inclusions from Venetia (Aulbach et al., 2002) and Kankan (Stachel et al., 2000a). Such anomalies indicate separation of Eu^{2+} from Eu^{3+} (and the other REE) and probably relate to plagioclase fractionation (or accumulation in the case of positive anomalies) during formation of crustal protoliths.

Additional support for the presence of "primary" trace element signatures comes from the observation of negative and positive Eu anomalies in eclogitic inclusions (garnet and clinopyroxene) in diamonds from Kankan (Guinea), Venetia (S.A.) and Namibia (Fig. 9). We therefore conclude that the trace element signature of eclogitic inclusions in diamonds is in support of crustal protoliths. The close spatial relationship of eclogitic diamonds to metasomatic veins (Schulze et al., 1996; Taylor et al., 2000) suggests that diamond precipitation occurred in the course of infiltration by fluids/melts, as it is the case for peridotitic sources.

4. Sublithospheric diamonds

4.1. Asthenosphere and transition zone

Compositional heterogeneities in the Earth's upper mantle are too large to employ the rather subtle compositional variations that are associated with the conversion of orthopyroxene to low-Ca clinopyroxene and of olivine to wadsleyite and ringwoodite for the recognition of deep asthenospheric and transition zone (410–660 km) inclusions (c.f. Stachel, 2001). Therefore, the evidence for diamond formation in the asthenosphere and the transition zone rests exclusively on the observation of inclusions of majorite garnet. With increasing depth pyroxene becomes soluble in the garnet structure (Ringwood, 1967) via simultaneous accommodation of four-valent and divalent cations on the octahedral garnet sites, resulting in the majorite end-member $M_6(Al_2M_1Si_1)^{[VI]}Si_6^{[IV]}O_{24}$. The majorite transition has a negative pressure–temperature slope (Fei and Bertka, 1999) and in particular the pressure dependence of the reaction is well established experimentally (e.g., Irifune, 1987). A second type of pressure-dependent substitution is $Na^{+}Si^{4+} = M^{2+}Al^{3+}$ (e.g., Irifune et al., 1989) which enables accommodation of the Na content of omphacitic clinopyroxene in majorite garnet.

The first find of majoritic garnet inclusions in diamonds was reported by Moore and Gurney (1985, 1989) for the Monastery Mine. Apart from scattered occurrences of single majorite inclusions, so far only three additional diamond sources with a significant proportion of majoritic garnet inclusions have been recognized: Jagersfontein (Deines et al., 1991) and the secondary deposits at Juina-São Luiz (Wilding, 1990; Harte, 1992; Hutchison, 1997; Kaminsky et al., 2001) and Kankan (Stachel et al., 2000a). The majority of majoritic garnet inclusions in diamonds have less than 6.4 Si atoms per formula unit which implies an origin well within the upper mantle (s.s.). However, diamonds from the four main deposits also contain inclusions which are likely to be derived from below 410 km, i.e., from the transition zone (e.g., Moore and Gurney, 1985, 1989; Deines et al., 1991).

Compositionally, almost all garnets containing a significant majorite component have eclogitic chemistries and show the same large spread in Ca contents observed for "normal" (lithospheric) eclogitic inclusions. More subtle compositional differences between lithospheric and sublithospheric eclogitic garnets are discussed in Stachel (2001).

Trace element data of majoritic garnet inclusions are scarce with the most detailed study being carried out by Moore et al. (1991) for the Monastery mine. Monastery garnets have relatively low LREE (0.02–2 times chondritic, Fig. 10) and high HREE (five out of seven majorites have 20–30 times chondritic HREE abundances). HREE show significant negative correlations with Si content (ranging from 6.23 to 6.58 cations). Two majoritic garnets from Kankan (Fig. 10) show a sharp rise from La_N to Ce_N and then flat or negative $LREE_N$–$HREE_N$ patterns (HREE at 10–30 times chondritic). For Kankan, two clinopyroxenes

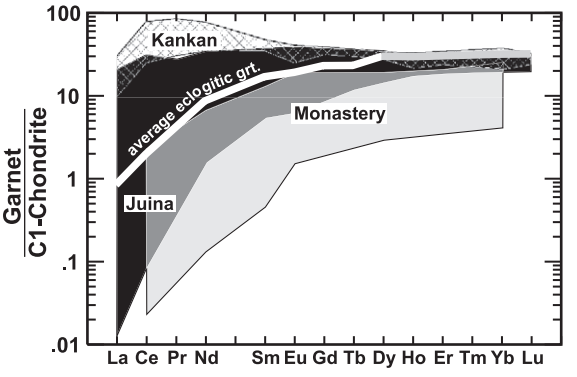

Fig. 10. Compositional fields for REE_N of majoritic (Si>6.15 cations at [O]=24) garnets from Monastery (seven diamonds), Juina-São Luiz (six diamonds) and Kankan (two diamonds). For references see Data base section in text. The average composition of lithospheric eclogitic garnet is taken from Fig. 7.

coexisting with majorite garnets have LREE contents of 100–400 times chondritic abundance (not shown), underlining the prominent LREE enrichment in this specific source. Majoritic eclogitic garnets from Juina-São Luiz are transitional in their LREE between Monastery and Kankan and enclose the average REE composition of "normal" eclogitic garnets (Fig. 10). Silicon contents for the garnets from Juina-São Luiz analyzed for trace elements (Wilding, 1990; Harte, 1992) range from 6.19 to 6.41 cations (indicating a purely asthenospheric origin) and REE from Ce onwards decrease with increasing Si.

In order to elucidate the origin of "basaltic" diamond sources in the asthenosphere and transition zone, Moore et al. (1991) applied garnet/melt partition coefficients to invert the REE composition of Monastery majorites into the composition of melts that may have been in equilibrium with such garnets. The resulting melts have negative $LREE_N/HREE_N$ slopes at high $LREE_N$, typical for low-volume mantle melts such as OIB, alkaline basalts and kimberlites. However, experimental data (Yurimoto and Ohtani, 1992; Draper et al., 2003), which only became available after the work of Moore et al. (1991), indicate that the partitioning behaviour of garnet/melt and majorite/melt is considerably different. Most notably, partition coefficients for HREE drop to values ≤ 1, with the opposite effect (a slight increase in partition coefficients) being observed for LREE. Thus, possible melts in equilibrium with Monastery garnets would have REE_N patterns which are fairly flat and less enriched compared to the results of Moore et al. (1991).

The coexistence of garnet and clinopyroxene in two diamonds from Kankan allows calculation of bulk rock REE_N patterns (assuming an approximate modal relationship of grt:cpx of 1:1) which show flat HREE at about 10–20 chondritic level but strong enrichment in LREE. The majority of Monastery garnets have similar HREE but much lower LREE and, therefore, a fairly flat REE_N pattern with $La_N/Yb_N < 1$ and $HREE_N$~10 may be predicted for the Monastery diamond source which is similar to normal MORB (see Fig. 8). A genetic link between subducted oceanic crust and formation of eclogitic diamonds in the asthenosphere and transition zone is also indicated by negative Eu anomalies in majoritic garnet and clinopyroxene included together in a diamond from Kankan (Fig. 11).

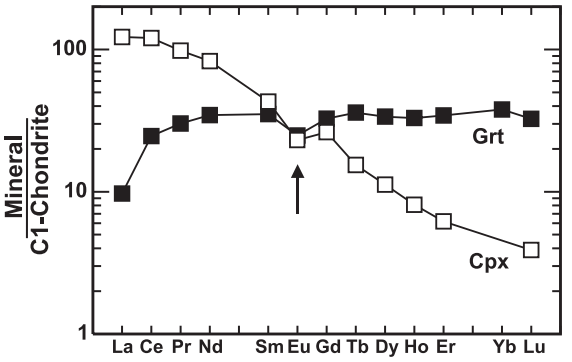

Fig. 11. Negative Eu anomalies in coexisting inclusions of majoritic garnet and clinopyroxene in diamond KK-81 from Kankan (Guinea).

4.2. Lower mantle

Harte et al. (1994) obtained the first trace element data for lower mantle inclusions discovered in diamonds from Rio São Luiz in the Juina area (Brazil). Since then, the data set for Juina-São Luiz has been expanded (Hutchison, 1997; Harte et al., 1999; Kaminsky et al., 2001) and additional REE analyses of lower mantle inclusions have become available for the Kankan deposits in Guinea (Stachel et al., 2000b).

Assuming a pyrolitic bulk composition, the mineralogy of the lower mantle will be dominated by MgSi–perovskite (>70%) and ferropericlase (almost 20%), with only minor amounts (about 8%) of CaSi–perovskite (Ringwood, 1991). For the top of the lower mantle (uppermost about 50 km), garnet is expected to be present as an additional phase, as the garnet–perovskite transition for pyrolitic bulk compositions takes place over a pressure interval, with garnet gradually dissolving in increasingly aluminous MgSi–perovskite (Irifune and Ringwood, 1987a; Wood, 2000). The role of tetragonal almandine–pyrope phase (TAPP; Harris et al., 1997) as a possible substitute for garnet in the topmost lower mantle is not entirely clear with both a possible important role of high ferric iron ratios in the source and an entirely retrograde origin being discussed (Finger and Conrad, 2000; Brenker et al., 2002).

Trace element data on inclusions in lower mantle diamonds (Harte et al., 1994, 1999; Stachel et al., 2000b) show that for lower mantle parageneses (incl.

TAPP), only CaSi–perovskite has to be considered as a significant depository of REE. This result has recently been confirmed experimentally by Wang et al. (2000a) and Corgne and Wood (2002). The presence of garnet, instead of TAPP, probably would require modification of this simplistic picture of CaSi–perovskite as the sole host of the lower mantle REE budget with respect to the HREE. Exsolution of CaSi–perovskite from majorite garnet begins in the deeper parts of the transition zone (Irifune and Ringwood, 1987b; Wood, 2000) and, therefore, garnet at the top of the lower mantle is not expected to contain significant Si^{4+} on octahedral sites, thus reducing electrostatic effects that lead to the suppressed compatibility of HREE in strongly majoritic garnets (see above).

REE_N patterns for CaSi–perovskite inclusions from Juina-São Luiz and Kankan are shown in Fig. 12. All inclusions have high $LREE_N/HREE_N$ and high LREE in common. Based on a modal proportion of 8% CaSi–perovskite in the lower mantle, Ce contents of 200–2000 times chondritic abundance (Fig. 12) indicate enrichment in the source rock to 10–100 the value of primitive mantle. Besides these common characteristics, on a more detailed level the REE_N patterns in Fig. 12 may be split into three groups, with both deposits (Juina-São Luiz and Kankan) being represented in all groups:

(1) A group of only two samples with REE patterns (shown as dotted lines in Fig. 12) that share the most extreme enrichment in LREE and consequently steep $LREE_N$–$HREE_N$ slopes. No significant changes in the slope of $MREE_N$ are associated with Eu (i.e., no Eu anomalies).
(2) A group of eight samples (solid lines in Fig. 12) that have flat $LREE_N$ at around 300–400 chondritic abundance. All samples in this group have positive Eu anomalies.
(3) A group of three samples (shown as dashed lines in Fig. 12) that share a "depletion" in MREE relative to the other CaSi–perovskites. All samples in this group have pronounced negative Eu anomalies.

REE_N patterns for samples in groups 1 and 3 were determined both by SIMS ("Kankan" and "Edinburgh") and by LA-ICP-MS ("Macquarie"), indicating that analytical uncertainties cannot be invoked to explain the observed Eu anomalies. Fractionation of Eu^{2+}/Eu^{3+} between lower mantle phases also is not a likely explanation (i) as the LREE–MREE budget of the lower mantle sources seems to be quantitatively

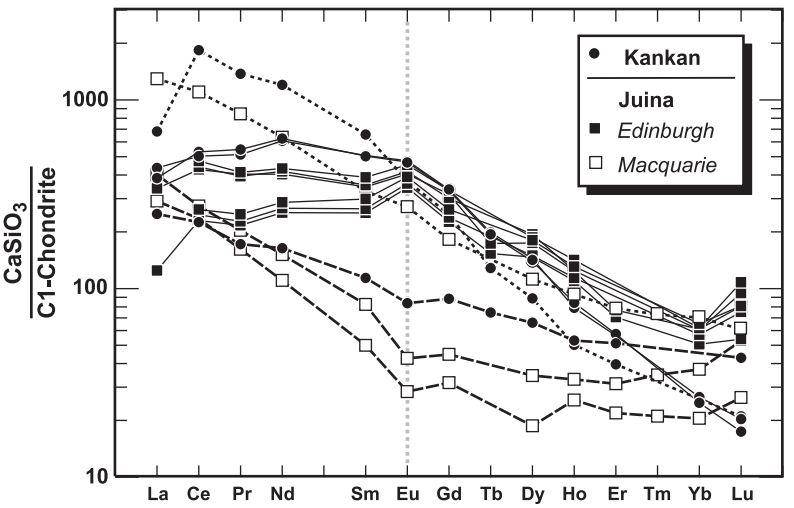

Fig. 12. REE_N patterns of $CaSiO_3$ inclusions in diamonds presumed to have originally crystallized in the lower mantle in the structure of CaSi–perovskite. For references see Data base section in text. The Kankan data and the "Edinburgh" portion of the Juina-São Luiz data set are ion probe analyses; the "Macquarie" data represent LA-ICP-MS analyses. Note that both methods are consistent with respect to Eu anomalies.

hosted in CaSi–perovskite and (ii) as other lower mantle phases do not show corresponding (“mirrored”) Eu anomalies (Harte et al., 1999; Stachel et al., 2000b).

CaSi–perovskites thus reflect source compositions that are highly enriched in incompatible trace elements and that may show positive or negative Eu anomalies. Combined with indications (low Al in MgSi–perovskite) that lower mantle diamonds are probably preferentially derived from the topmost part of the lower mantle, a relationship to former oceanic slabs which accumulated at the top of the lower mantle (megalith model of Ringwood, 1991) appears likely (Harte et al., 1999; Stachel et al., 2000b).

In such a subduction scenario, negative Eu anomalies could indicate a protolith that experienced plagioclase fractionation (e.g., volcanic rocks in the upper part of oceanic crust), whereas positive anomalies would indicate feldspar accumulation (cumulate rocks in gabbroic reservoirs). In two cases (Kankan: KK-66a and 87a), positive Eu anomalies are accompanied by extreme concentrations in Sr (about 7000 ppm), which would be consistent with a cumulate model. However, lack of knowledge about possible variations in the modal composition of the lower mantle sources and in particular about the presence or absence of garnet, make a detailed evaluation of the different types of REE_N patterns in CaSi–perovskites impossible. In addition, the possibility exists that instead of diamond formation in ancient slabs, the enriched REE patterns (including Eu anomalies) were imprinted on “normal” lower mantle rocks during metasomatic alteration through slab derived fluids and melts.

In any case, it appears that diamond formation beneath the lithosphere (asthenosphere, transition zone and lower mantle) is intimately linked to subduction processes. Oxygen fugacity in the sublithospheric mantle is expected to decrease with increasing pressure for crystallochemical reasons (O’Neill et al., 1993; Wood et al., 1996), which may lead to conditions that are too reducing for the formation of macro diamonds. In such a scenario former crustal rocks may form a necessary prerequisite providing the redox gradients necessary for diamond precipitation in an otherwise reduced sublithospheric mantle.

Acknowledgements

The data set presented in this review only exists because of continuous generous support through De Beers Consolidated Mines who supplied all the diamonds from which the inclusions were analyzed by us and provided financial assistance for costly ion probe work. The ion probe facility at Edinburgh University and in particular the outstanding support of John Craven and Richard Hinton was instrumental in carrying out most of the research reviewed here. T.S. is grateful to Ben Harte (Edinburgh) for first introducing him to the interpretation of REE in mantle minerals and his continued advise (including numerous reviews). Grants by Deutsche Forschungsgemeinschaft (DFG), NSERC and the Canada Research Chairs Program are gratefully acknowledged. John Gurney and an anonymous reviewer are thanked for their constructive criticisms of the manuscript.

References

Aulbach, S., Stachel, T., Viljoen, K.S., Brey, G.P., Harris, J.W., 2002. Eclogitic and websteritic diamond sources beneath the Limpopo Belt—is slab-melting the link? Contrib. Mineral. Petrol. 143, 56–70.

Brenker, F.E., Stachel, T., Harris, J.W., 2002. Exhumation of lower mantle inclusions in diamond: ATEM investigation of retrograde phase transitions, reactions and exsolution. Earth Planet. Sci. Lett. 198, 1–9.

Burgess, S.R., Harte, B., 1999. Tracing lithospheric evolution trough the analysis of heterogeneous G9/G10 garnets in peridotite xenoliths: I. Major element chemistry. In: Gurney, J.J., Gurney, J.L., Pascoe, M.D., Richardson, S.H. (Eds.), The J.B. Dawson Volume, Proceedings of the VIIth International Kimberlite Conference. Red Roof Design, Cape Town, pp. 66–80.

Cartigny, P., Harris, J.W., Phillips, D., Girard, M., Javoy, M., 1998. Subduction-related diamonds? The evidence for a mantle-derived origin from coupled $\delta^{13}C-\delta^{15}N$ determinations. Chem. Geol. 147, 147–159.

Corgne, A., Wood, B.J., 2002. $CaSiO_3$ and $CaTiO_3$ perovskite-melt partitioning of trace elements: implications for gross mantle differentiation. Geophys. Res. Lett. 29 (art. no. 1933). doi:10.1029/2001GL014398.

Davies, R.M., Griffin, W.L., O’Reilly, S.Y., Doyle, B.J., 2004. Mineral inclusions and geochemical characteristics of microdiamonds from the DO27, A154, A21, A418, DO18, DD17 and Ranch Lake kimberlites at Lac de Gras, Central Slave Craton, Canada. Lithos, these proceedings.

Deines, P., Harris, J.W., Gurney, J.J., 1991. The carbon isotopic composition and nitrogen content of lithospheric and asthenospheric diamonds from the Jagersfontein and Koffiefontein

kimberlitev, South Africa. Geochim. Cosmochim. Acta 55, 2615–2625.

Doroshev, A.M., Brey, G.P., Girnis, A.V., Turkin, A.I., Kogarko, L.N., 1997. Pyrope–knorringite garnets in the Earth's upper mantle: experiments in the $MgO–Al_2O_3–SiO_2–Cr_2O_3$ system. Russ. Geol. Geophys. 38, 559–586.

Draper, D.S., Xirouchakis, D., Agee, C.B., 2003. Trace element partitioning between garnet and chondritic melt from 5 to 9 GPa: implications for the onset of the majorite transition for the Martian mantle. Phys. Earth Planet. Inter. 139, 149–169.

Farquhar, J., et al., 2002. Mass-independent sulfur of inclusions in diamond and sulfur recycling on early Earth. Science 298 (5602), 2369–2372.

Fei, Y., Bertka, C.M., 1999. Phase transitions in the Earth's mantle and mantle mineralogy. In: Fei, Y., Bertka, C.M., Mysen, B.O. (Eds.), Mantle Petrology: Field Observations and High-Pressure Experimentation. A Tribute to Francis R. (Joe) Boyd. Special Publication. The Geochemical Society, Houston, pp. 189–207.

Finger, L.W., Conrad, P.G., 2000. The crystal structure of "tetragonal almandine–pyrope phase" (TAPP): a reexamination. Am. Mineral. 85, 1804–1807.

Frank, F.C., 1969. Diamonds and deep fluids in the upper mantle. In: Runcorn, S.K. (Ed.), The Application of Modern Physics to the Earth's and Planetary Interiors. Wiley, New York, pp. 247–250.

Frey, F.A., Green, D.H., 1974. The mineralogy, geochemistry and origin of lherzolite inclusions in Victorian basanites. Geochim. Cosmochim. Acta 38, 1023–1059.

Griffin, W.L., O'Reilly, S.Y., Ryan, C.G., 1999a. The composition and origin of subcontinental lithospheric mantle. In: Fei, Y., Bertka, C.M., Mysen, B.O. (Eds.), Mantle Petrology: Field Observations and High Pressure Experimentation: A Tribute to Francis R. (Joe) Boyd. Special Publication. The Geochemical Society, Houston, pp. 13–45.

Griffin, W.L., Shee, S.R., Ryan, C.G., Win, T.T., Wyatt, B.A., 1999b. Harzburgite to lherzolite and back again: metasomatic processes in ultramafic xenoliths from the Wesselton kimberlite Kimberley, South Africa. Contrib. Mineral. Petrol. 134 (2–3), 232–250.

Grütter, H.S., Sweeney, R.J., 2000. Tests and constraints on single-grain Cr-pyrope barometer models: some initial results. GAC-MAC GeoCanada 2000 Conference, Calgary, 2000. CD, not paginated.

Gurney, J.J., 1984. A correlation between garnets and diamonds in kimberlites. Publ.-Geol. Dept. Univ. Ext., Univ. West. Aust. 8, 143–166.

Gurney, J.J., 1989. Diamonds. In: Ross, J., et al. (Eds.), Kimberlites and Related Rocks. Spec. Publ.-Geol. Soc. Aust., vol. 14. Blackwell, Carlton, pp. 935–965.

Harris, J.W., Hutchison, M.T., Hursthouse, M., Light, M., Harte, B., 1997. A new tetragonal silicate mineral occurring as inclusions in lower-mantle diamonds. Nature 387 (6632), 486–488.

Harris, J.W., Stachel, T., Léost, I., Brey, G.P., 2004. Peridotitic diamonds from Namibia: constraints on the composition and evolution of their mantle source. Lithos 77, 209–223 (this volume).

Hart, S., Dunn, T., 1993. Experimental cpx/melt partitioning of 24 trace elements. Contrib. Mineral. Petrol. 113, 1–8.

Harte, B., 1992. Trace element characteristics of deep-seated eclogite parageneses—an ion microprobe study of inclusions in diamonds. V.M. Goldschmidt Conference. The Geochemical Society, Reston, VA, p. A-48.

Harte, B., Kirkley, M.B., 1997. Partitioning of trace elements between clinopyroxene and garnet: data from mantle eclogites. Chem. Geol. 136, 1–24.

Harte, B., Hutchison, M.T., Harris, J.W., 1994. Trace element characteristics of the lower mantle: an ion probe study of inclusions in diamonds from São Luiz, Brazil. Min. Mag. 58A, 386–387.

Harte, B., Harris, J.W., Hutchison, M.T., Watt, G.R., Wilding, M.C., 1999. Lower mantle mineral associations in diamonds from Sao Luiz, Brazil. In: Fei, Y., Bertka, C.M., Mysen, B.O. (Eds.), Mantle Petrology: Field Observations and High Pressure Experimentation: A Tribute to Francis R. (Joe) Boyd. Special Publication. The Geochemical Society, Houston, pp. 125–153.

Hoal, K.E.O., Hoal, B.G., Erlank, A.J., Shimizu, N., 1994. Metasomatism of the mantle lithosphere recorded by rare-earth elements in garnets. Earth Planet. Sci. Lett. 126, 303–313.

Hutchison, M.T., 1997. Constitution of the deep transition zone and lower mantle shown by diamonds and their inclusions. Unpubl. PhD thesis, University of Edinburgh, vol. 1. 340 pp., vol 2. 306 pp.

Ireland, T.R., Rudnick, R.L., Spetsius, Z., 1994. Trace elements in diamond inclusions from eclogites reveal link to Archean granites. Earth Planet. Sci. Lett. 128, 199–213.

Irifune, T., 1987. An experimental investigation of the pyroxene–garnet transformation in a pyrolite composition and its bearing on the constitution of the mantle. Earth Planet. Sci. Lett. 45, 324–336.

Irifune, T., Ringwood, A.E., 1987a. Phase transformations in a harzburgite composition to 26 GPa: implications for dynamical behaviour of subducting slab. Earth Planet. Sci. Lett. 86, 365–376.

Irifune, T., Ringwood, A.E., 1987b. Phase transformations in primitive MORB and pyrolite compositions to 25 GPa and some geophysical implications. In: Manghnani, M., Syono, Y. (Eds.), High Pressure Research in Geophysics. AGU, Washington, pp. 231–242.

Irifune, T., Hibberson, W.O., Ringwood, A.E., 1989. Eclogite–garnetite transformation at high pressure and its bearing on the occurrence of garnet inclusions in diamond. In: Ross, J., et al. (Eds.), Kimberlites and Related Rocks. Spec Publ.-Geol. Soc. Aust., vol. 14. Blackwell, Carlton, pp. 877–882.

Jacob, D.E., Foley, S.F., 1999. Evidence for Archean ocean crust with low high field strength element signature from diamondiferous eclogite xenoliths. Lithos 48, 317–336.

Kaminsky, F.V., et al., 2001. Superdeep diamonds from the Juina area, Mato Grosso State, Brazil. Contrib. Mineral. Petrol. 140, 734–753.

Kirkley, M.B., Gurney, J.J., Otter, M.L., Hill, S.J., Daniels, L.R., 1991. The application of C isotope measurements to the identification of the sources of C in diamonds—a review. Appl. Geochem. 6, 477–494.

Luth, R.W., 1993. Diamonds, eclogites, and the oxidation state of the Earth's mantle. Science 261 (5117), 66–68.

Macgregor, I.D., Manton, W.I., 1986. Roberts-Victor eclogites—ancient oceanic-crust. J. Geophys. Res.-Solid Earth Planets 91 (B14), 14063–14079.

McCandless, T.E., Gurney, J.J., 1997. Diamond eclogites: comparison with carbonaceous chondrites, carbonaceous shales, and microbial carbon-enriched MORB. Geol. Geofiz. 38 (2), 371–381.

McDonough, W.F., Sun, S.-S., 1995. The composition of the Earth. Chem. Geol. 120, 223–253.

Moore, R.O., Gurney, J.J., 1985. Pyroxene solid solution in garnets included in diamonds. Nature 318, 553–555.

Moore, R.O., Gurney, J.J., 1989. Mineral inclusions in diamond from Monastery kimberlite, South Africa. In: Ross, J., et al. (Eds.), Kimberlites and Related Rocks. Spec. Publ.-Geol. Soc. Aust., vol. 14. Blackwell, Carlton, pp. 1029–1041.

Moore, R.O., Gurney, J.J., Griffin, W.L., Shimizu, N., 1991. Ultrahigh pressure garnet inclusions in Monastery diamonds—trace element abundance patterns and conditions of origin. Eur. J. Mineral. 3, 213–230.

Nielson, J.E., Wilshire, H.G., 1993. Magma transport and metasomatism in the mantle: a critical review of current models. Am. Mineral. 78, 1117–1134.

O'Neill, H.S.C., 1980. An experimental study of the iron–magnesium partitioning between garnet and olivine and its calibration as a geothermometer: corrections. Contrib. Mineral. Petrol. 72, 337.

O'Neill, H.S.C., Wood, B.J., 1979. An experimental study of the iron–magnesium partitioning between garnet and olivine and its calibration as a geothermometer. Contrib. Mineral. Petrol. 70, 59–70.

O'Neill, H.S.C., et al., 1993. Mössbauer spectroscopy of mantle transition zone phases and determination of minimum Fe^{3+} content. Am. Mineral. 78, 456–460.

Ringwood, A.E., 1967. The pyroxene garnet transformation in the Earth's mantle. Earth Planet. Sci. Lett. 2, 255–263.

Ringwood, A.E., 1991. Phase transformations and their bearing on the constitution and dynamics of the mantle. Geochim. Cosmochim. Acta 55 (8), 2083–2110.

Schulze, D.J., Wiese, D., Steude, J., 1996. Abundance and distribution of diamonds in eclogite revealed by volume visualization of CT X-ray scans. J. Geol. 104, 109–114.

Schulze, D.J., Harte, B., Valley, J.W., Brenan, J.M., Channer, D.M.D., 2003. Extreme crustal oxygen isotope signatures preserved in coesite in diamond. Nature 423 (6935), 68–70.

Shimizu, N., 1975. Rare earth elements in garnets and clinopyroxenes from garnet lherzolite nodules in kimberlites. Earth Planet. Sci. Lett. 25, 26–32.

Shimizu, N., Richardson, S.H., 1987. Trace element abundance patterns of garnet inclusions in peridotite-suite diamonds. Geochim. Cosmochim. Acta 51, 755–758.

Shimizu, N., Sobolev, N.V., Yefimova, E.S., 1997. Chemical heterogeneities of inclusion garnets and juvenile character of peridotitic diamonds from Siberia. Russ. Geol. Geophys. 38-2, 356–372.

Sobolev, N.V., Lavrent'ev, Y.G., Pokhilenko, N.P., Usova, L.V., 1973. Chrome-rich garnets from the kimberlites of Yakutia and their paragenesis. Contrib. Mineral. Petrol. 40, 39–52.

Sobolev, N.V., et al., 1998. Extreme chemical diversity in the mantle during eclogitic diamond formation: Evidence from 35 garnet and 5 pyroxene inclusions in a single diamond. Int. Geol. Rev. 40 (7), 567–578.

Stachel, T., 2001. Diamonds from the asthenosphere and the transition zone. Eur. J. Mineral. 13, 883–892.

Stachel, T., Harris, J.W., 1997a. Diamond precipitation and mantle metasomatism—evidence from the trace element chemistry of silicate inclusions in diamonds from Akwatia, Ghana. Contrib. Mineral. Petrol. 129 (2–3), 143–154.

Stachel, T., Harris, J.W., 1997b. Syngenetic inclusions in diamond from the Birim field (Ghana)—a deep peridotitic profile with a history of depletion and re-enrichment. Contrib. Mineral. Petrol. 127 (4), 336–352.

Stachel, T., Viljoen, K.S., Brey, G., Harris, J.W., 1998. Metasomatic processes in lherzolitic and harzburgitic domains of diamondiferous lithospheric mantle: REE in garnets from xenoliths and inclusions in diamonds. Earth Planet. Sci. Lett. 159 (1–2), 1–12.

Stachel, T., Harris, J.W., Brey, G.P., 1999. REE patterns of peridotitic and eclogitic inclusions in diamonds from Mwadui (Tanzania). In: Gurney, J.J., Gurney, J.L., Pascoe, M.D., Richardson, S.H. (Eds.), The P.H. Nixon Volume, Proceedings of the VIIth International Kimberlite Conference. Red Roof Design, Cape Town, pp. 829–835.

Stachel, T., Brey, G.P., Harris, J.W., 2000a. Kankan diamonds (Guinea) I: From the lithosphere down to the transition zone. Contrib. Mineral. Petrol. 140, 1–15.

Stachel, T., Harris, J.W., Brey, G.P., Joswig, W., 2000b. Kankan diamonds (Guinea) II: Lower mantle inclusion parageneses. Contrib. Mineral. Petrol. 140, 16–27.

Stachel, T., Harris, J.W., Aulbach, S., Deines, P., 2002. Kankan diamonds (Guinea) III: $\delta^{13}C$ and nitrogen characteristics of deep diamonds. Contrib. Mineral. Petrol. 142 (4), 465–475.

Stachel, T., Viljoen, K.S., McDade, P., Harris, J.W., 2004. Diamondiferous lithospheric roots along the western margin of the Kalahari Craton—the peridotitic inclusion suite in diamonds from Orapa and Jwaneng. Contrib. Mineral. Petrol. 147, 32–47.

Tappert, R., et al., 2004. Mineral inclusions in diamonds from the Panda kimberlite, Slave Province, Canada. Eur. J. Mineral. (submitted).

Taylor, L.A., et al., 1996. Eclogitic inclusions in diamonds: evidence of complex mantle processes over time. Earth Planet. Sci. Lett. 142 (3–4), 535–551.

Taylor, L.A., et al., 2000. Diamonds and their mineral inclusions, and what they tell us: a detailed "pull-apart" of a diamondiferous eclogite. Int. Geol. Rev. 42, 959–983.

Van Orman, J.A., Grove, T.L., Shimizu, N., Layne, G.D., 2002. Rare earth element diffusion in a natural pyrope single crystal at 2.8 GPa. Contrib. Mineral. Petrol. 142, 416–424.

Wang, W.Y., Gasparik, T., 2001. Metasomatic clinopyroxene inclusions in diamonds from the Liaoning province, China. Geochim. Cosmochim. Acta 65 (4), 611–620.

Wang, W., Sueno, S., Takahashi, E., 1998. Influence of Cr on REE partitioning between garnet and silicate melt: application to metasomatism of mineral inclusions in diamonds. Rev. High Press. Sci. Technol. 7, 92–94.

Wang, W.Y., Gasparik, T., Rapp, R.P., 2000a. Partitioning of rare earth elements between $CaSiO_3$ perovskite and coexisting phases: constraints on the formation of $CaSiO_3$ inclusions in diamonds. Earth Planet. Sci. Lett. 181, 291–300.

Wang, W.Y., Sueno, S., Takahashi, E., Yurimoto, H., Gasparik, T.,

2000b. Enrichment processes at the base of the Archean lithospheric mantle: observations from trace element characteristics of pyropic garnet inclusions in diamonds. Contrib. Mineral. Petrol. 139, 720–733.

Wilding, M.C., 1990. Untitled. Unpubl. PhD thesis, thesis, University of Edinburgh, UK. 281 pp.

Wood, B.J., 2000. Phase transformations and partitioning relations in peridotite under lower mantle conditions. Earth Planet. Sci. Lett. 174, 341–351.

Wood, B.J., Pawley, A., Frost, D.R., 1996. Water and carbon in the Earth's mantle. Philos. Trans.-Royal Soc., Math. Phys. Eng. Sci. 354, 1495–1511.

Wyllie, P.J., 1987. Metasomatism and fluid generation in mantle xenoliths. In: Nixon, P.H. (Ed.), Mantle Xenoliths. Wiley, Chichester, pp. 609–621.

Yurimoto, H., Ohtani, E., 1992. Element partitioning between majorite and liquid—a secondary ion mass-spectrometric study. Geophys. Res. Lett. 19, 17–20.

Zack, T., Foley, S.F., Jenner, G.A., 1997. A consistent partition coefficient set for clinopyroxene, amphibole and garnet from laser ablation microprobe analysis of garnet pyroxenites from Kakanui New Zealand. Neues Jahrb. Mineral. Abh. 172 (1), 23–41.